

Adaptive control method and experimental study of cone crusher based on aggregate online detection

Huaiying Fang^{1,2}, Xiaosheng Ji¹, Jianhong Yang¹, Yuxuan Yang³, Tianchen Ji¹, Chaoming Wei³

¹ School of Mechatronics and Automation, Huaqiao University, Xiamen 361021, China

² Fujian Key Laboratory of Green Intelligent Drive and Transmission for Mobile Machinery, Xiamen 361021, China

³ Fujian Southern Road Machinery Co., Ltd, Quanzhou 362021, China

Corresponding author: happen@hqu.edu.cn (Huaiying Fang)

Abstract: The size of the discharge outlet of a cone crusher directly impacts the size of the aggregate produced. However, the discharge outlet is still adjusted manually, which has a significant error and affects production efficiency. For this reason, this study proposed an adaptive control method for cone crushers based on aggregate online detection. Firstly, the aggregate image was segmented using an instance segmentation model and the anchor and structure of the model were optimised. Then, this study proposed an evaluation method for quickly and accurately assessing the overall segmentation effect of network models. By comparing the results with those before optimisation, the accuracy of the optimised network model was improved from 0.923 to 0.940. Finally, an adaptive control experiment was conducted based on the online aggregate detection results. The experimental results showed that the discharge particle size distribution of the cone crusher becomes more stable after intelligent control is added, with the variance of the proportion of cumulative gradation at 15 mm decreased from 34.3 to 14.4. These results indicated that the developed adaptive control system effectively controls the fine processing of coarse aggregates and significantly improves the quality of aggregate crushing and processing.

Keywords: cone crusher, coarse aggregate, instance segmentation, gradation, intelligent control

1. Introduction

With the rapid development of industrial technology, the mining industry has been increasing its mining efforts, placing higher demands on crushing equipment (Ma et al., 2020). A cone crusher is a machine that performs a series of hammer-like blows on the aggregate in the crushing chamber to reduce it to a finer fraction (Wills and Finch, 2015; Hulthén and Evertsson, 2009). It is widely used in mining, construction materials, and other industries. Compared to other crushing equipment, cone crushers have the advantages of a high reduction ratio, low energy consumption, high production efficiency, and uniform product size (Yamashita et al., 2021; Purohit et al., 2021). It is usually arranged at the back end of the crushing process and plays a crucial role in the crushing size of the final product. However, during the production process, the cone crusher experiences liner wear, fluctuations in the output of the parent material, changes in pressure retention capacity, and other impacts. These factors result in changes to the aggregate gradation (Airikka, 2015), necessitating the prompt adjustment of the discharge outlet. Currently, the adjustment of the discharge outlet of cone crushers still relies on manual operations, which are complex and prone to significant errors without data support. These issues hamper production efficiency and increase the risk of damage to components such as bearings and gears, which can further impact production (Cheng and Liu, 2014; Itävuo and Vilkkö, 2021; You, 2018). Therefore, there is a need to explore a more scientific and intelligent way to adjust the discharge outlet of cone crushers (Vasilyeva et al., 2023).

The rapid development of aggregate online detection technology provides a new method for the online adjustment of the cone crusher. In 2015, Bagheri et al. analysed the particle shape of irregular particles using calliper measurements, image analysis, laser scanning and scanning electron microscopy, respectively, and proposed a new method based on the projected area of particles for measuring the length of particles in three-dimensional dimensions (Bagheri et al., 2015). In 2021, Yang et al. (2021) proposed a method to analyse the image of recycled concrete coarse aggregate in a stacked state based on the improved watershed algorithm. They introduced threshold segmentation and distance transform distribution to identify and segment the particle edges of the recycled coarse aggregate in a stacked state and achieved better segmentation results. In 2021, Hu et al. (2021) segmented coarse aggregate images of different particle sizes, materials, and gradations using deep learning and traditional watershed methods. The experimental results showed that the deep learning algorithm had higher accuracy in coarse aggregate image segmentation than traditional watershed methods, and it also demonstrated better robustness in situations with water and mud. In 2022, Xu et al. (2022) proposed a mineral recognition algorithm for rock flakes based on a deep learning method. They used deep learning algorithms for the segmentation and recognition of different minerals in rocks and experimentally proved that deep learning algorithms were more accurate than traditional image segmentation methods. The above research indicates that the deep learning algorithm is more advantageous than the conventional image segmentation algorithm. However, deep learning algorithms have yet to be applied to actual working conditions or used to carry out the online adjustment of the discharge outlet of the cone crusher.

Many studies have proposed different control methods for intelligent control of cone crushers. In 2011, Hulthén and Evertsson (2011) proposed an algorithm for real-time control of a cone crusher, with a particular focus on the two critical variables of the cone crusher, the closed-edge setting and the eccentric speed, which were adjusted in real-time to improve the efficiency and quality of production. In 2016, Guo et al. (2016) proposed a control method based on an absolute value encoder to improve the control accuracy of the discharge outlet of a multi-cylinder hydraulic cone crusher, which uses the absolute value encoder to measure the number of rotational revolutions of the movable cone and adjusts the discharge outlet to the set value according to the data processing and logic operation. In 2018, Mykhailenko et al. (2018) proposed an adaptive control method based on a nonlinear prediction model, which improved the crushing efficiency and product quality of the cone crusher by integrally considering key factors such as the physical properties of the ore, the structural parameters of the crusher, and the working conditions. In 2020, Xie (2020) studied the multi-cylinder cone crusher system, used the soft measurement method based on the least squares mechanism vector machine to detect the ore particle size, and proposed a machine learning method based on a neural network to set the target value of crushed stone particle size, to achieve intelligent control switching for different working conditions and production requirements. In 2021, Wang (2021) developed an intelligent feeding control system for the crushing process that reduces the impact of feeding on the cone crusher's production, thereby enhancing its production stability and service life. In 2022, Grishin et al. (2022) proposed an intelligent control-oriented approach. They demonstrated this by using a camera to monitor the discharge outlet, distinguishing frame differences in the video stream to detect defects and wear in the crusher liner, and applying fuzzy logic theory and the fuzzy set approach for intelligent control. The above studies demonstrate the potential application of intelligent control methods in the field of cone crushers and have achieved some results. However, they lack the capability for online adjustment, which leaves the stable grading of production aggregates unguaranteed.

To address the online control issue of discharge gradation in cone crushers, this study combined the online detection of aggregates with intelligent control of the cone crusher. We proposed a self-adaptive control method based on online aggregate detection and developed an intelligent control system for the cone crusher. Reflecting actual working conditions, we constructed an experimental platform, proposed an evaluation method for coarse aggregate segmentation, and optimised the neural network structure to address issues within coarse aggregate segmentation. As a result, we improved the segmentation accuracy of the coarse aggregate image. Subsequently, we implemented the adaptive control of the cone crusher, centered on the online detection of gradation. Our results validated the effectiveness of this adaptive control method when applied to cone crushers.

2. Experimental equipment and methods

2.1. Experimental equipment

The intelligent control system of the cone crusher is shown in Fig. 1, which mainly consists of an area scan camera, a conveyor belt, LED lights, a distance sensor, an edge computer, and a cone crusher.

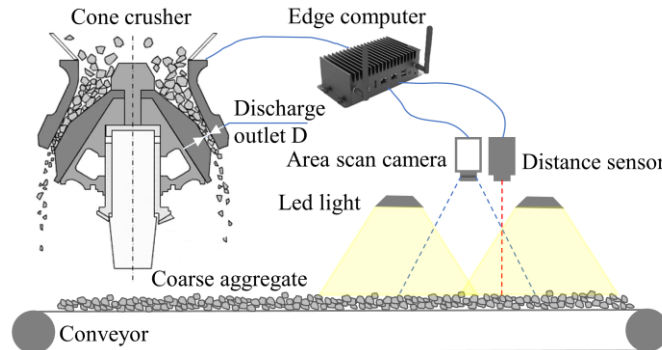


Fig. 1. Intelligent control system for cone crushers

The coarse aggregate, crushed by the cone crusher, is transported to the inspection area on the conveyor belt. An area scan camera is placed directly above the conveyor belt to capture the coarse aggregate image from a vertical perspective. LED lights are arranged above the belt to provide uniform illumination, minimizing the impact of aggregate shadow on image segmentation. A distance sensor measures the aggregate thickness aligned with each image. Lastly, an edge computer processes these images to determine gradation and implement adaptive control of the cone crusher.

2.2. Aggregate online detection methods

Traditional methods for the online detection of aggregates encompass the watershed algorithm and its variants (Bai et al., 2021; Qiu et al., 2017; Wang et al., 2018), along with laser scanning, scanning electron microscopy (Bagheri et al., 2015), and other techniques. However, the practical application of techniques such as laser scanning and scanning electron microscopy is significantly constrained, as they are only suitable for detecting discrete aggregates. The watershed algorithm and its enhanced versions require adjustment of numerous parameters. Their robustness, therefore, leaves room for improvement and is easily compromised by environmental disturbances. Compared to traditional image processing methods, the instance segmentation algorithm employed in this study demonstrates superior accuracy and robustness. Furthermore, it effectively circumvents the common issues of over-segmentation and under-segmentation encountered with the watershed algorithm.

2.2.1. Instance segmentation network models

Instance segmentation is an accurate segmentation of foreground and background in an image based on target detection, which can accurately segment each separate object or individual and obtain its contour information. The objective of this study is to use an instance segmentation model to segment the images of coarse aggregates. This will allow us to obtain the 2D shape of each aggregate, which we can then use for statistical analysis of gradation (Zhang et al., 2023).

As shown in Fig. 2, the model adopts the backbone (Resnet-50 (He et al., 2016) + FPN (Lin et al., 2017)) network architecture to process the coarse aggregate image and obtain the feature map. Then, the preset anchors are used on the feature map to generate proposals through the region proposal network (RPN). To get the fixed-size feature map (FSFM) for each proposal, the model uses Roi Align's method to crop and resize the feature map. After that, each FSFM is further processed by mask head and box head to obtain mask, coordinates, and category information for each proposal. Finally, instance segmentation results are obtained based on this information.

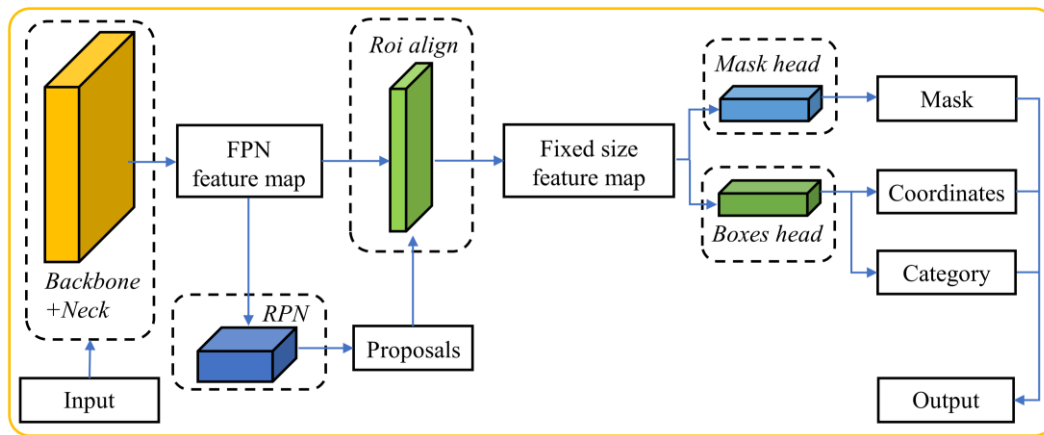


Fig. 2. Network model structure

The original model resulted in a noticeable degree of under-segmentation during the segmentation of aggregate images. Therefore, optimising the network model is imperative to enhance its suitability and effectiveness for coarse aggregate image segmentation.

2.2.2. Optimisation of instance segmentation network models

While the commonly used Mask R-CNN network model boasts commendable generalizability, it requires further optimization when applied specifically to the context of aggregate detection, based on an aggregate dataset. In this study's network model for generating proposals on five feature maps, multiple anchors are pre-defined on each feature map, as shown in Fig. 3(a). However, the default sizes of these anchors do not align well with the characteristics of the aggregate dataset. Therefore, the K-Means clustering algorithm was employed in this experiment to adjust the ratios and sizes of the anchors.

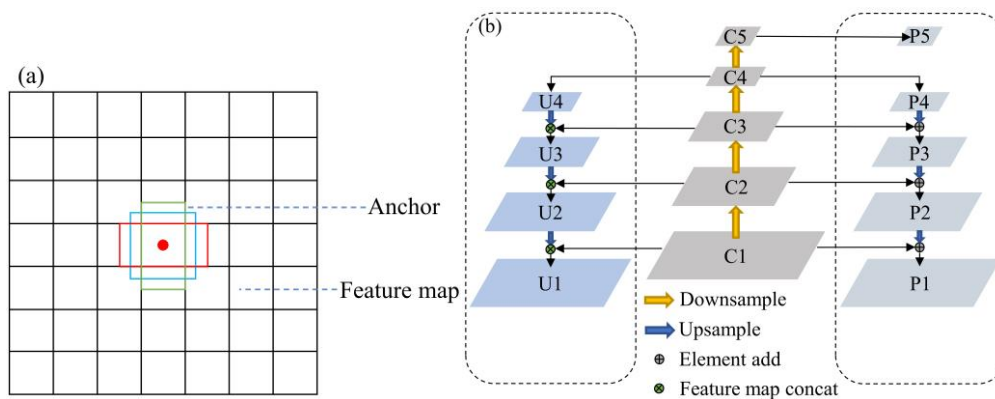


Fig. 3. Schematic representation of the improvement of the network model. (a) Anchor diagram; (b) Schematic diagram of the improved Backbone

The K-Means clustering algorithm process is as follows:

- (1) Determine the value of K. Use clustering to divide the dataset into K sets.
- (2) Select K data points randomly from the dataset to serve as the initial centroids.
- (3) Calculate the distance from each data point in the dataset to the K centroids. Assign each data point to the cluster of the nearest centroid.
- (4) After all the data points have been assigned to clusters, recompute the centroids for each of the K clusters.
- (5) If the centroids do not change, or if the shift in their position is below a certain threshold, consider the clustering to have achieved the desired result and terminate the algorithm.
- (6) If the centroid changes or if the magnitude of change exceeds a certain threshold, repeat steps (3)-(5).

During ratio clustering with 3 cluster centres and using the Manhattan distance formula, the conversion of ratios to radians can be calculated according to equation (1).

$$r = \text{atan}\left(\frac{h}{\omega}\right) \quad (1)$$

Where h is the height of the aggregate, ω is the width of the aggregate.

After feature extraction and enhancement, the feature maps sent to RPN consist of 5 sizes. Therefore, when performing size clustering, there are 5 cluster centres. The distance formula used is equation (2).

$$f(\omega_1, h_1, \omega_2, h_2) = 1 - \frac{\min(\omega_1, \omega_2) \times \min(h_1, h_2)}{(\omega_1 \times h_1) + (\omega_2 \times h_2) - \min(\omega_1, \omega_2) \times \min(h_1, h_2)} \quad (2)$$

Cluster the size according to the obtained fixed ratio and change the formula to equation (3).

$$g(\omega_1, h_1, s) = \min\left(f(\omega_1, h_1, \frac{s}{\sqrt{r_i}}, s \times r_i)\right) \quad (3)$$

where s is the cluster centre size, r_i is the i -th ratio.

The stacking effect of the coarse aggregate image in the stacked state compared with the discrete coarse aggregate image will lead to blurring of the image, and the crucial information will be easily lost when downsampling using the backbone network, which affects the accuracy of the instance segmentation. To solve this problem, we used a combination of U-Net (Ronneberger et al., 2015) and Mask R-CNN (He et al., 2017) to improve the backbone network. The encoding part of U-Net mainly consists of convolutional and maximum pooling layers, while the decoding part consists of upsampling and skip connections. The role of skip connections is to fuse deep and shallow features to retain more information. U-Net uses channel splicing for information fusion, which preserves more dimensional information for better image detail. The feature pyramid network (FPN) of Mask R-CNN uses the addition of channel elements to achieve multi-scale feature fusion, especially for small target detection. Combining U-Net and Mask R-CNN can more effectively address the challenges posed by stacked coarse aggregate images, significantly reducing information loss (Tian et al., 2020).

The improved backbone structure is shown in Fig. 3(b). The input image is first processed using Resnet-50 to obtain a total of five feature maps with different sizes: C1, C2, C3, C4 and C5. Then introduce the FPN structure, process these feature maps, and get five FPN feature maps of P1, P2, P3, P4, and P5. On this basis, implement upsampling and channel splicing operations from C4, resulting in four U-Net feature maps: U1, U2, U3, and U4. These operations correspond to the decoding part of the U-Net, where the size of the feature maps is restored to the size of the original input image by the upsampling operation, and the deep and shallow features are fused by channel splicing.

After the improved backbone network, the image will get two sets of feature maps: the U-Net feature map and the FPN feature map. As shown in Fig. 4, the U-Net feature map undergoes Roi Align operation to get FSFM, and then it is passed to the mask head for foreground and background segmentation to generate the mask of the image. Meanwhile, the FPN feature map also undergoes Roi Align operation to get FSFM. Then, it is passed to the box head for classification and regression to obtain the coordinates and category information of the objects in the image. Finally, by combining mask, coordinates and category, an instance segmentation image of the coarse aggregate is constituted. This new network structure is called U-Mask, which combines U-Net and Mask R-CNN to fully utilise the feature fusion capability of U-Net and the object detection capability of Mask R-CNN.

2.2.3. Calculation method of gradation

Due to the irregular shape of the two-dimensional projection surface of the coarse aggregate, an equivalent method is usually employed to represent the particle size of the coarse aggregate. We chose the area perimeter method for particle size calculation in this experiment. The definition of this method is four times the ratio of the area to the perimeter of a particle, as shown in equation (4).

$$P_s = \frac{4S}{L} \quad (4)$$

where S is the area of the projection surface, L is the perimeter of the projection surface.

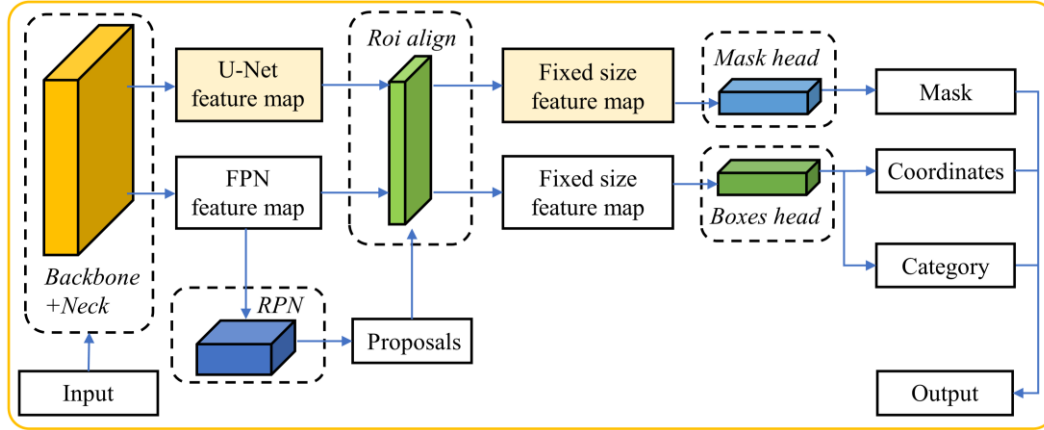


Fig. 4. U-Mask network structure

The traditional method of calculating gradation is to calculate the percentage of each particle size grade by the mass ratio of each sieve on each layer. However, when using the coarse aggregate image method for gradation calculation, we can only obtain two-dimensional information about the aggregate and observe the coarse aggregate on the surface, which requires a reasonable gradation calculation method. In this experiment, we choose the area method as the grading calculation method (Maiti et al., 2017). The area method takes the ratio of the area of each grain size to the total area as the percentage of that grain size. The calculation formula is shown in equation (5).

$$P_{si} = \frac{S_i}{S} \quad (5)$$

where S is the sum of the projected areas of all aggregates, S_i is the sum of the projected areas of aggregates with particle size in the i -th particle size class.

2.2.4. Evaluation methods

In most datasets, the performance of algorithms is usually measured using mean average precision (MAP). This metric evaluates the accuracy of segmentation based on the intersection over union (IOU) between the predicted and ground truth bounding boxes. If the IOU is greater than a set threshold, the segmentation is considered correct; otherwise, the segmentation is considered incorrect. However, MAP predominantly focuses on the accuracy of the detected bounding boxes and overlooks the size of the objects, which restricts it from fully and accurately describing the precision of coarse aggregate image segmentation. Therefore, this paper proposes a new evaluation index for the problem of coarse aggregate image segmentation. This index introduces the contour IOU (CIOU) concept to evaluate a single aggregate's segmentation quality. The CIOU metric represents the intersection and ratio of overlap between the ground truth contour of the coarse aggregate and the segmentation contour yielded by the model for the same aggregate. The calculation formula is shown in Equation (6).

$$CIOU = \frac{Intersection}{Union} \quad (6)$$

where *Intersection* is the area of the intersection part of the overlap of two contour regions, *Union* is the area of the concatenation part of the overlap of two contour regions.

To provide a comprehensive evaluation of the coarse aggregate segmentation quality across the entire image, it is necessary to obtain and assign weights to the area size of each coarse aggregate. This weighting process facilitates a more accurate representation of the importance of various coarse aggregates in the cumulative segmentation results. The computation formula for this process is demonstrated in Equation (7).

$$MCIOU = \frac{\sum_{i=1}^n CIOU_i \times S_i}{\sum_{i=1}^n S_i} \quad (7)$$

where S_i is the area of the overlapping concatenation of the i -th region.

When the mean contour intersection over union (MCIU) between the predicted aggregate contour by the model and the manually annotated aggregate contour is higher, it indicates that their overlapping parts are larger and the predicted aggregate contour by the model is closer to the one manually annotated. Therefore, the segmentation quality is better.

3. Experimental results and discussion

3.2. Network model optimisation experiments

In the original model, the default sizes of anchors are set to [32, 64, 128, 256, 512], and the ratios are [0.5, 1, 2]. After analysing the data using the K-Means clustering algorithm, a new set of anchor sizes [22, 47, 81, 134, 195] and ratios [0.7, 1, 1.5] is obtained, as shown in Table 1.

Table 1. Each feature map anchor

Feature layer	Original anchor		Improved anchor	
	Sizes	Aspect ratio	Sizes	Aspect ratio
P1	32		22	
P2	64		47	
P3	128	[0.5, 1, 2]	81	[0.7, 1, 1.5]
P4	256		134	
P5	512		195	

Comparing the training results of Mask R-CNN, K- Mask (K-Means + Mask R-CNN) and K- U-Mask (K-Means + U-Mask R-CNN). As can be seen from the curves in Fig. 5, the K- U-Mask has the fastest improvement in accuracy and has a higher final accuracy than the Mask R-CNN. This result is because the network model needs to learn the anchor centre point offset and the length and width scaling. Proper anchor settings can make learning the regression task easier for the RPN and box head. By applying the K-Means clustering algorithm, we obtain an anchor that better matches the distribution of the dataset, thus reducing the loss of the network model in bounding box regression. In addition, K- U-Mask introduces a network structure for semantic segmentation, which provides more information to the foreground-background segmentation task than the simple summation of individual elements on the feature map in FPN. This improvement contributes to reducing information loss and enhancing the accuracy of segmentation.

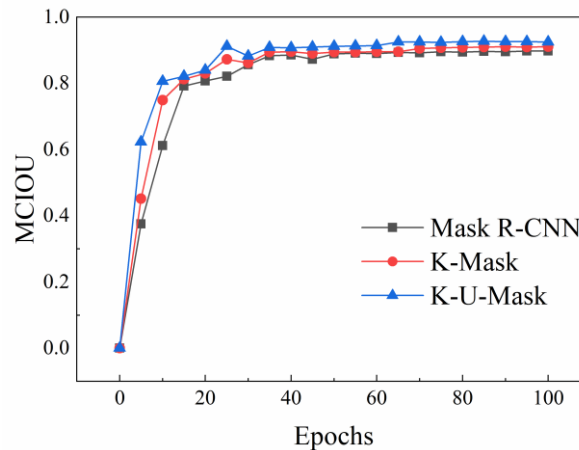


Fig. 5. The MCIU training curve

The coarse aggregate image was segmented using the network before and after optimisation, respectively, and the segmentation results are shown in Fig. 6. Comparing Fig. 6(a) with Fig. 6(b) unmistakably showcases that employing the K-Means clustering algorithm for anchor settings enables the detection of a larger number of objects within the model, with particular efficacy in pinpointing tiny targets. This is evidenced by the instances within the white dashed region in Fig. 6(b). The comparison

of Fig. 6(b) and Fig. 6(c) reveals that the coarse aggregate segmentation image appears more completely after incorporating the semantic segmentation network architecture. This suggests that the improved network enhances the segmentation accuracy of coarse aggregate contours, as indicated by the white dashed region in Fig. 6(c).

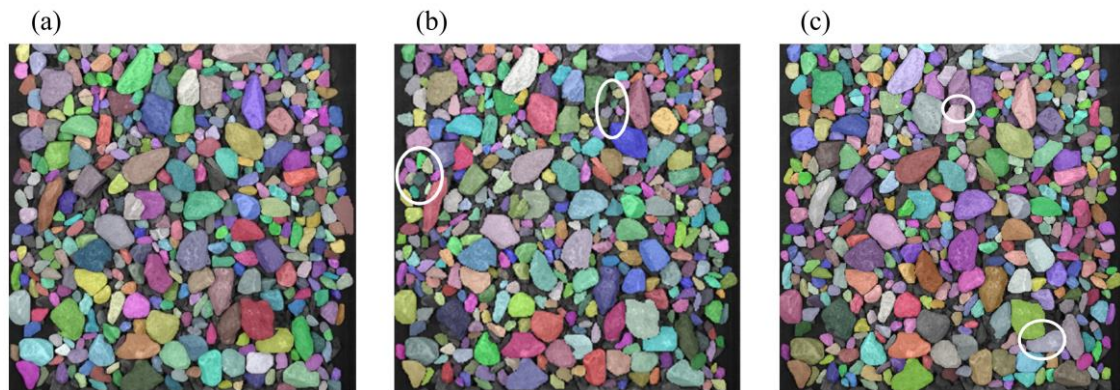


Fig. 6. Segmentation image of different network models. (a) Segmented image of Mask R-CNN; (b) Segmented image of K-Mask; (c) Segmented image of K-U-Mask

The comparison of the evaluation index in Table 2 demonstrates the significant improvement of K-U-Mask over Mask R-CNN. Through the improvement of the model, the evaluation index MCIU is improved from 0.923 to 0.940, and this improvement is due to the addition of semantic segmentation to K-U-Mask, which makes the model able to reduce the misclassification of fuzzy outline pixel points, thus reducing the under-segmentation and over-segmentation problems to a certain extent, and this also fully proves the effectiveness of the improved algorithm proposed in this paper in the field of coarse aggregate image segmentation.

Table 2. Evaluation index

Network model	Mask R-CNN	K- Mask	K-U-Mask
MCIU	0.923	0.930	0.940

3.3. Cone crusher intelligent control experiment

3.2.1. Segmentation experiment with different discharge outlets

Intelligent control of the cone crusher based on the gradation online detection method requires testing the accuracy of the model, which proves that there are apparent differences in the proportion of cumulative gradation curves detected under different discharge outlet sizes. For this reason, we set the discharge outlet size to 22 mm and 20 mm for crushing production and compared the coarse aggregate images and the proportion of cumulative gradation curves produced, as shown in Fig. 7. The coarse aggregate particle size produced when the discharge outlet size is 22 mm is significantly larger than that produced when the discharge outlet size is 20 mm. This indicates that the discharge outlet size substantially affects the coarse aggregate size produced by the cone crusher. Meanwhile, this study used the instance segmentation model to segment the coarse aggregate images with different discharge outlet sizes and achieved the desired results. Whether the discharge outlet size is 22 mm or 20 mm, the model can complete the segmentation of the coarse aggregate image very well, which meets the needs of practical use.

The cone crusher was subjected to continuous online testing for 1 hour at 22 mm and 20 mm discharge outlets, and the statistical results are plotted in Fig. 8. It can be observed from the Fig. that the proportion of cumulative gradation of each aggregate size is higher at discharge outlet size 20 mm than at discharge outlet size 22 mm. It shows a clear difference in the proportion of cumulative gradation curves and matches the production situation. The effectiveness of online detection of coarse aggregate image segmentation based on deep learning is verified, and the feasibility of intelligent control of cone crusher based on the online detection method of gradation is also proved.

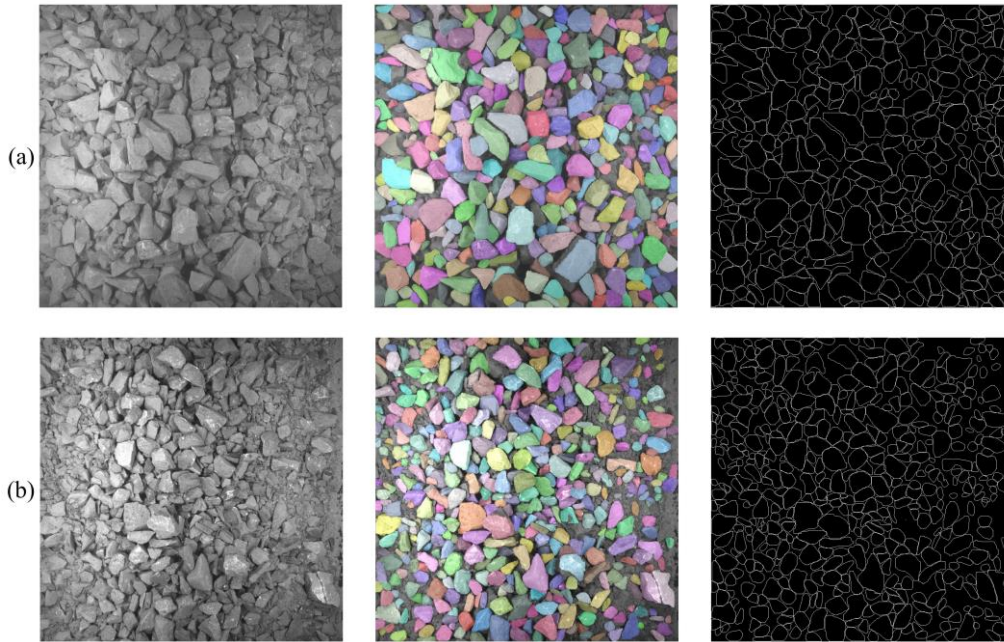


Fig. 7. The production situation and image of different discharge outlet sizes. (a) Discharge outlet 22 mm: original image (left), segmented image (middle), boundary image (right); (b) Discharge outlet 20 mm: original image (left), segmented image (middle), boundary image (right)

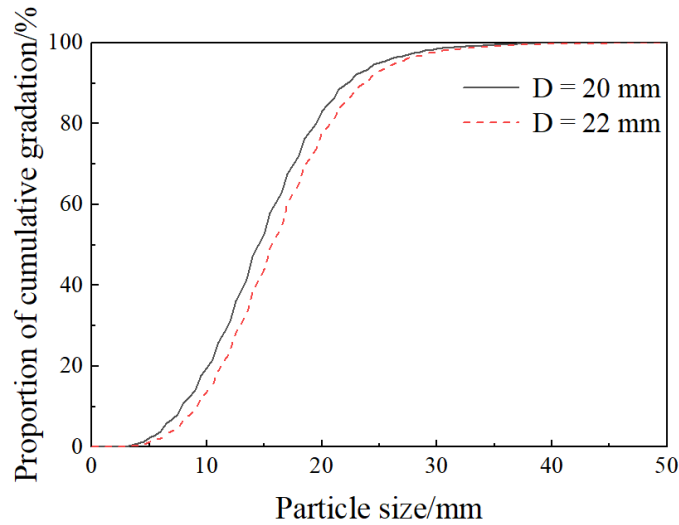


Fig. 8. The proportion of cumulative gradation curves for different discharge outlets

3.2.2. Segmentation experiment with different material thickness

In the production process of cone crusher, the height of the crushing chamber material level has an essential impact on the crushing effect, and the high material level can achieve adequate crushing. At the same time, the thickness of coarse aggregate on the conveyor belt is also affected by the level of the crushing chamber. As the level of the crushing chamber increases, the thickness of the coarse aggregate on the conveyor belt will also become larger. These two changes will lead to changes in the collected coarse aggregate image, resulting in different proportions of cumulative gradation curves calculated when the same discharge size is produced. To investigate the effect of cone crusher throughput on the grade curve, we installed a distance sensor on the top of the inspection box. The higher the height of the material level in the crushing chamber, the greater the thickness of the coarse bone on the conveyor belt and the smaller the value of the signal collected by the distance sensor. On the contrary, when the material level is lower, the signal value collected by the distance sensor is larger.

To investigate the effect of material thickness on the gradation data, the discharge outlet size is set constant, and the crushing production of the cone crusher is tracked for one day; 7295 coarse aggregate images are collected in real-time using the detection system for segmentation, and the distance sensor value corresponding to each image is collected for measuring the coarse aggregate thickness. By averaging the distance sensor values collected each minute, we obtained the curve of coarse aggregate thickness over time (as illustrated in Fig. 9(a)). This curve reveals significant fluctuations during the cone crusher's production process, characterized by multiple spur phenomena. This phenomenon indicates that the thickness of the coarse aggregate on the conveyor belt is relatively small at these moments. To eliminate the influence of the spurs on the results, it is necessary to set a threshold value to screen the data from the distance sensor. When the value of the distance sensor exceeds the threshold, the grading data for the corresponding image is not counted.

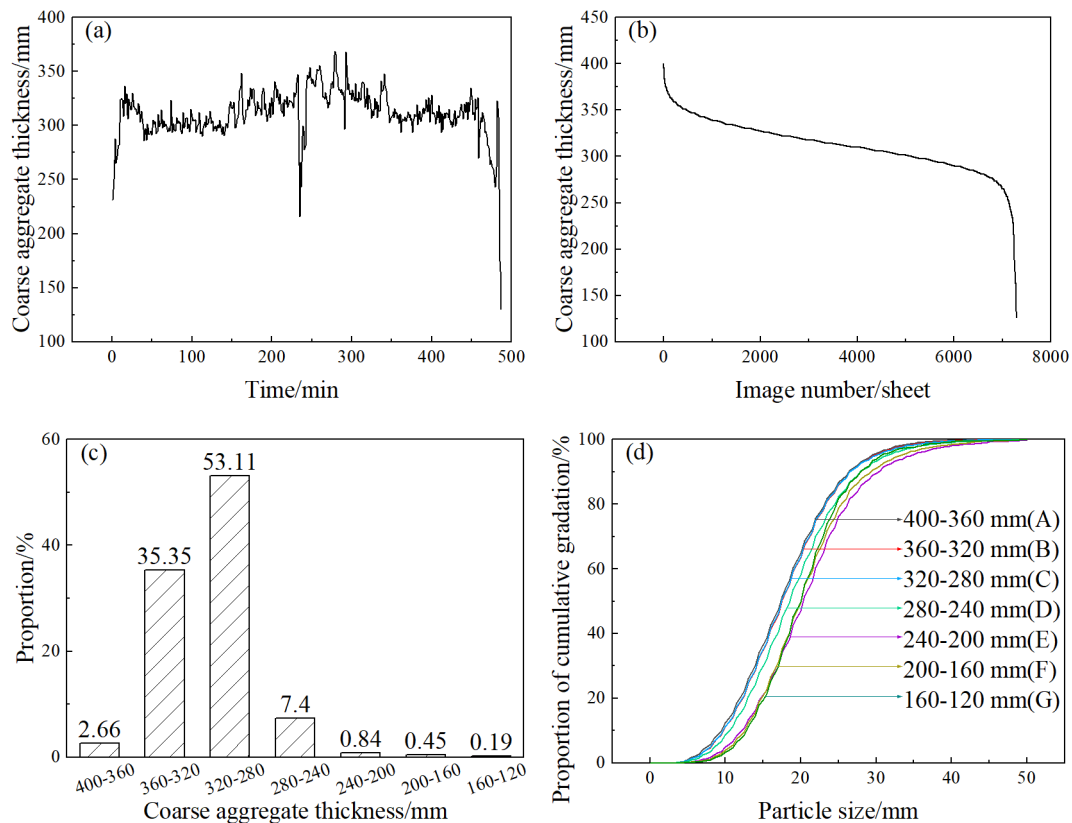


Fig. 9. Proportion of cumulative gradation curves of different thicknesses. (a) Thickness variation curve; (b) Thickness distribution curve; (c) Proportion of different aggregate thicknesses; (d) Proportion of cumulative gradation curves for different aggregate thicknesses

To determine the size of the threshold, we analysed the thickness statistics of 7295 coarse aggregate images, with the results depicted in Fig. 9(b). The thickness of the coarse aggregate is distributed in the range of 120–400 mm, and the segmentation is carried out at intervals of 40 mm. The percentage of each interval is shown in Fig. 9 (c). Segmentation and proportion of cumulative gradation statistics of coarse aggregate images with different thicknesses are performed, and the results are shown in Fig. 9(d). Fig. 9(d) shows that when the coarse aggregate's thickness is 280–400 mm, the difference in the proportion of cumulative gradation of each particle size is slight, and the proportion of cumulative gradation curves A, B, and C almost overlap. In contrast, the proportion of cumulative gradation curves C, D and E show that the proportion of cumulative gradation of each particle size starts to decrease after the thickness of the coarse aggregate is lower than a particular value. Moreover, when the thickness of coarse aggregate is too low (curves E, F, G), the change of proportion of cumulative gradation curves has no apparent pattern. This suggests that within the crushing chamber when the height of the material level drops below a certain threshold, the particle size of the coarse aggregate experiences significant variations. This is because when the material level of coarse aggregate in the crushing chamber is too low, the

extrusion is not sufficient, and the degree of crushing is not enough, resulting in a larger particle size. Considering that curves D, E, F and G account for a small percentage, and most of these data were collected within half an hour of the start of production (when the level of coarse aggregate in the crushing chamber is low), they cannot be used as a basis for adjustment under normal working conditions. The effect of coarse aggregate segmentation with different thicknesses is shown in Fig. 10, and it can also be seen in Figs. 10(b) and 10(c) that when the coarse aggregate level is too low, the aggregate size produced by the cone crusher is large. Therefore, we set 280 mm as the threshold value, and when the material level is lower than this threshold value, the grading data of the corresponding pictures will not be counted. At the same time, the average height of the material level in half an hour will be determined, and when it is lower than the threshold value, the size of the discharge outlet of the cone crusher will not be adjusted.

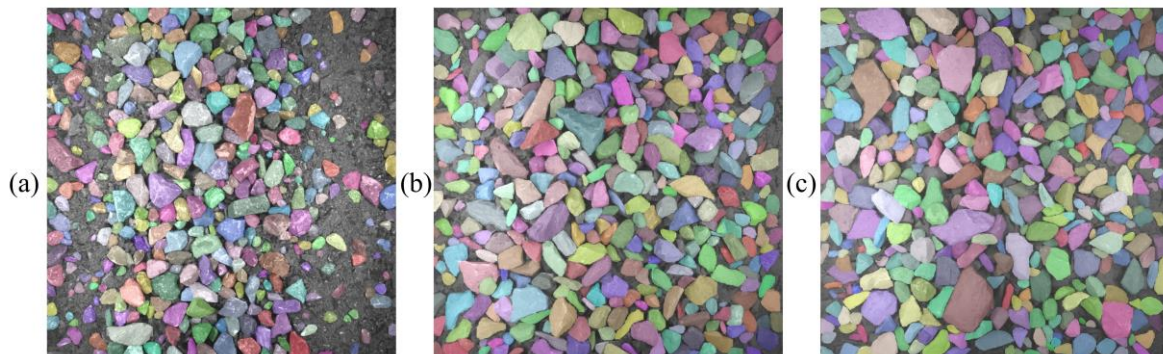


Fig. 10. Segmented image with different coarse aggregate thickness. (a) Segmented image at a thickness of 320-280 mm; (b) Segmented image at a thickness of 280-240 mm; (c) Segmented image at a thickness of 240-200 mm

4. Discharge outlet intelligent control experiment

Intelligent control of the cone crusher based on the online detection of the gradation needs to find the key points of the gradation curve, detect the changes in the proportion of cumulative gradation at the key points and feedback control the discharge outlet of the cone crusher to adjust accordingly, the control flow chart is shown in Fig. 11. Before and after adjusting the discharge outlet several times, the trend of the difference in the proportion of cumulative gradation at different key points is the same, but the average value and the fluctuation amplitude are different, as shown in Fig. 12(a). To achieve a sensitive and stable adjustment of the cone crusher, it is required that the average value of the difference in the proportion of cumulative gradation at the key points before and after adjusting the discharge outlet several times is larger and the standard deviation is smaller. To assess the stability of the regulation effect, we use the coefficient of variation as a judgement criterion. The coefficient of variation is calculated as shown in equation (8). As shown in Fig. 12(b), a smaller coefficient of variation is preferable.

$$c_v = \frac{\sigma}{\mu} \quad (8)$$

where c_v is the coefficient of variation, σ is the standard deviation, and μ is the mean.

Fig. 12(b) shows that the variation coefficient reaches the minimum value at 15 mm, indicating the proportion of cumulative gradation at 15 mm as the optimal key point for intelligent control. The proportion of cumulative gradation data at 15 mm was counted for seven consecutive hours, and the results are shown in Fig. 13. The normal production of this aggregate batch requires the proportion of cumulative gradation at 15 mm to be between 47.6% and 64.3%. However, in the manual control group, the proportion of cumulative gradation at 15 mm is mostly below 47.6%, leading to an oversized particle size of the produced aggregate. This is because the manual control group lacks clearly defined standards and relies only on experience to adjust when the aggregate size increases significantly. As a result, nearly half of the time between the two adjustments, the produced aggregates did not meet the requirements and had quality problems. In contrast, in the intelligent control group, the proportion of cumulative gradation at 15 mm was usually within the normal production range. When the proportion

of cumulative gradation at the key point is less than the set parameter, the discharge outlet of the cone crusher will be reduced by 1 mm immediately so that the aggregate produced in the next stage will return to normal. It can also be seen from Table 3 that the average value of the proportion of cumulative gradation at 15 mm of the intelligent control group is within the normal range and fluctuates less than that of the manual control group, which further proves the effectiveness of the intelligent control using the proportion of cumulative gradation at 15 mm as the key point.

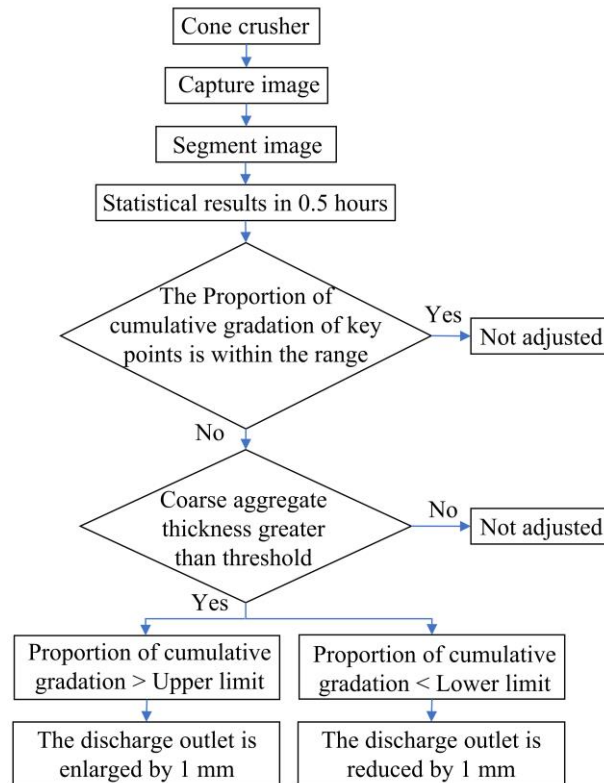


Fig. 11. Cone crusher intelligent control flowchart

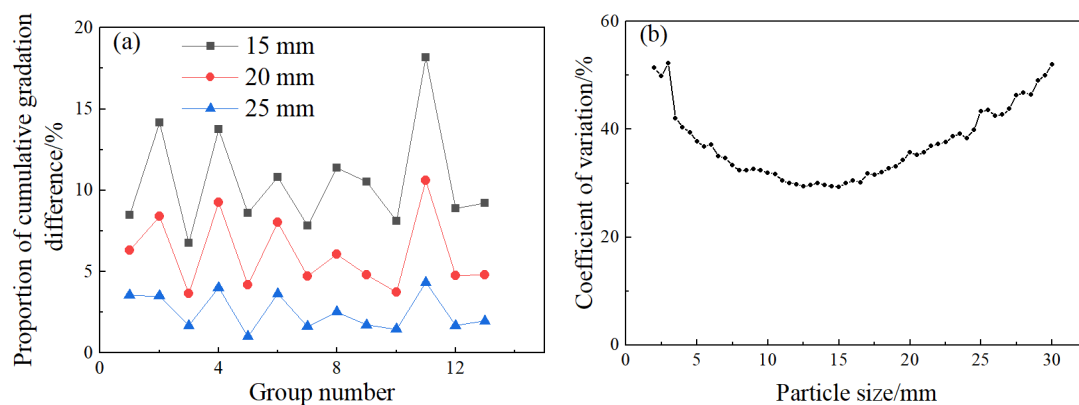


Fig. 12. Proportion of cumulative gradation difference curve and coefficient of variation. (a) Proportion of cumulative gradation difference curve; (b) Coefficient of variation of the difference in proportion of cumulative gradation

Table 3. Mean and variance of the proportion of cumulative gradation at 15 mm in 7 hours

Experimental group	Mean value (%)	Variance
Manual control of discharge outlet	46.39	34.3
Intelligent control of discharge outlet	53.5	14.4

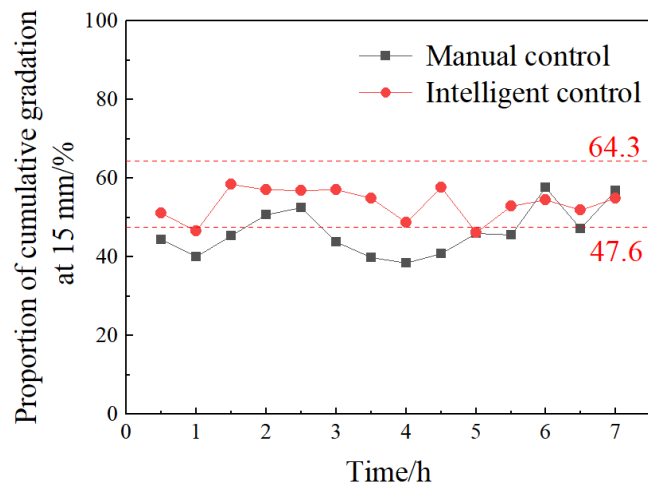


Fig. 13. Comparison chart of the proportion of cumulative gradation at 15 mm

5. Conclusions

To realise the online detection and intelligent control of the discharge gradation of the cone crusher, this study proposes a method of adaptive control of the cone crusher based on the online detection of gradation and develops the intelligent control system of cone crusher and draws the following conclusions.

(1) The application of the instance segmentation model can accurately segment the coarse aggregate image under the actual stacking condition to realise the online detection of coarse aggregate gradation, and the experiment proves that the segmentation algorithm based on deep learning can achieve the segmentation effect to meet the production requirements in the actual production of cone crusher.

(2) The evaluation method proposed in this study can easily and quickly evaluate the overall segmentation effect of network models and help compare the performance of different models.

(3) Optimising the anchor in Mask R-CNN by the K-Means algorithm can improve the anchor distribution and data mismatch problems. In addition, applying the U-Net idea to optimise the network can alleviate the information loss problem of the neural network and further improve the segmentation accuracy.

(4) This study applied the online inspection and control system to the actual production of the cone crusher. The experiment proves that the size of the discharge outlet significantly affects the coarse aggregate particle size produced by the cone crusher, and it is feasible to carry out intelligent control of the cone crusher based on the online inspection method of gradation.

(5) The trend of the difference in the proportion of cumulative gradation at different key points is the same. However, the average value and fluctuation amplitude are different, and it is effective to select the optimal key points for adaptive control of the cone crusher, which can control the coarse aggregate size and reduce the fluctuation of the size.

In this study, a timed adjustment of 1 mm was used to control the discharge outlet size of the cone crusher. However, when the particle size of the coarse aggregate differs greatly from the target requirement, it may require multiple adjustments. Subsequent studies can track the data and build a control model based on the current and target states for faster adjustment.

Acknowledgments

The authors give thanks to the financial support of Quanzhou High-level Talent Team Introduction Project (2023CT003) and Pilot Project of Fujian Province (2023Y0026).

References

AIRIKKA, P., 2015. *Automatic feed rate control with feed-forward for crushing and screening processes*. IFAC-PapersOnLine, 48(17), 149-154.

- BAGHERI, G.H., BONADONNA, C., MANZELL, I., VONLANTHEN, P., 2015. *On the characterization of size and shape of irregular particles*. Powder Technol. 270, 141-153.
- BAI, F.Y., FAN, M.Q., YANG, H.L., DONG, L., 2021. *Image segmentation method for coal particle size distribution analysis*. Particuology, 56, 163-170.
- CHENG, L.X., LIU, G.X., 2014. *Design and improvement of automatic control system of cone crusher*. Xinjiang Nonferrous Met. 37 (5), 81-82.
- GRISHIN, I.A., BOCHKOV, V.S., VELIKANOV, V.S., DYORINA, N.V., SUROVTSOV, M.M., MOREVA, Y.A., 2022. *Implementing a discharge slot width control system in cone crushers*. Vestnik of Nosov Magnitogorsk State Technical University, 20(2), 13-22.
- GUO, S., JIAN, H.F., DU, Z.B., 2016. *Design and implementation on controlling discharge port of crusher with encoder*. Min. & Process. Equip. 44 (11), 45-49.
- HE, K., GKIOXARI, G., DOLLÁR, P., GIRSHICK, R., 2017. *Mask R-CNN*. In Proceedings of the IEEE International Conference on Computer Vision (ICCV), pp. 2961-2969.
- HE, K., ZHANG, X., REN, S., SUN, J., 2016. *Deep residual learning for image recognition*. In Proceedings of the IEEE conference on computer vision and pattern recognition, pp. 770-778.
- HU, X., 2023. *Measurement and characterization of coarse aggregate morphology based on predicted void content*. Huaqiao Univ.
- HULTHÉN, E., EVERTSSON, C.M., 2009. *Algorithm for dynamic cone crusher control*. Minerals Engineering, 22(3), 296-303.
- HULTHÉN, E., EVERTSSON, C.M., 2011. *Real-time algorithm for cone crusher control with two variables*. Minerals Engineering. 24(9), 987-994.
- ITÁVUO, P., VILKKO, M., 2021. *Size reduction control in cone crusher*. Miner. Eng. 173, 107202.
- LIN, T.Y., DOLLÁR, P., GIRSHICK, R., HE, K., HARIHARAN, B., BELONGIE, S., 2017. *Feature pyramid networks for object detection*. In Proceedings of the IEEE conference on computer vision and pattern recognition, pp. 2117-2125.
- MA, L.F., WU, F.B., PAN, W.Q., 2020. *Research status and development trend of cone crusher*. Heavy Mach. 5, 9-13.
- MAITI, A., CHAKRAVARTY, D., BISWAS, K., HALDER, A., 2017. *Development of a mass model in estimating weight-wise particle size distribution using digital image processing*. Int. J. Min. Sci. Technol. 27, 435-443.
- MYKHAILENKO, O., SHCHOKIN, V., SHCHOKINA, O., 2018. *Adaptive control of the ore crushing process in cone crushers based on nonlinear predictive model*. Univ. Publ. Petroșani.
- PUROHIT, N.L., SHARMA, A., 2021. *Cone crushing industries enhance performance using controlling and monitoring*. International Journal, 6(3).
- QIU, R., ZHU, R.X., XU, H.K., 2017. *Image segmentation algorithm based on improved watershed algorithm*. J. Jilin Univ. (Sci. Ed.), 55(03), 629-634.
- RONNEBERGER, O., FISCHER, P., BROX, T., 2015. *U-Net: Convolutional networks for biomedical image segmentation*. In International Conference on Medical Image Computing and Computer-Assisted Intervention, pp. 234-241.
- TIAN, Y.N., YANG, G.D., WANG, Z., LI, E., LIANG, Z., 2020. *Instance segmentation of apple flowers using the improved mask R-CNN model*. Biosyst. Eng. 193, 64-278.
- VASILYEVA, N., GOLYSHEVSKAIA, U., SNIATKOVA, A., 2023. *Modeling and improving the efficiency of crushing equipment*. Symmetry, 15(7), 1343.
- WANG, H.T., 2021. *Development and application of intelligent ore feeding control system in crushing process*. Copper Proj. 04, 71-74.
- WANG, R., ZHANG, W., SHAO, L., 2018. *Research of ore particle size detection based on image processing*. In Proceedings of 2017 Chinese Intelligent Systems Conference: Volume II, pp. 505-514.
- WILLS, B.A., FINCH, J., 2015. *Wills' mineral processing technology: an introduction to the practical aspects of ore treatment and mineral recovery*. Butterworth-Heinemann, Oxford, England.
- XIE, X.D., 2020. *Study on intelligent control system of multi-cylinder hydraulic cone crusher*. Shenyang Univ. Technol.
- XU, S.J., SU, C., ZHU, K.Y., ZHANG, X.C., 2022. *Automatic identification of mineral in petrographic thin sections based on images using a deep learning method*. J. Zhejiang Univ. (Sci. Ed.), 49(6), 743-752.
- YAMASHITA, A.S., THIVIERGE, A., EUZÉBIO, TAM., 2021. *A review of modeling and control strategies for cone crushers in the mineral processing and quarrying industries*. Miner. Eng. 170, 107036.
- YANG, Z.Q., YANG, J., XIONG, W.Y., 2021. *Practical method for identifying morphological information of recycled coarse aggregate bulk based on watershed algorithm*. J. Chin. Ceram. Soc. 49(08), 1691-1698.

- YOU, C.T., 2018. *Design of automatic control system for single-cylinder hydraulic cone crusher*. J. Shandong Ind. Technol. 2, 116-116.
- ZHANG, R., LI, K., YU, F., ZHANG, H., GAO, Z., HUANG, Y., 2023. *Aggregate particle identification and gradation analysis method based on the deep learning network of Mask R-CNN*. Mater. Today Commun. 35, 106269.